

# A multiplicative finite strain formulation for void growth models using elastic correctors

Meijuan Zhang<sup>a</sup>, Guadalupe Vadillo<sup>b</sup>, Francisco Javier Montáns<sup>a,\*</sup>

<sup>a</sup>*E.T.S.I Aeronautica y del Espacio, Pl. del Cardenal Cisneros, 3, 28040 Madrid, Spain*

<sup>b</sup>*E.T.S.I Caminos Canales y Puertos, Cl. Profesor Aranguren, 3, 28040 Madrid, Spain*

---

## Abstract

The proposed work is a formulation for large-strain non-isochoric plastic deformation, using the GTN yield function as the void growth rule as an example. This formulation is fully hyperelastic and uses the Kroner-Lee multiplicative decomposition. It adopts the concept of elastic correctors, and thus, does not have any constraints on the amount of elastic strain or the form of elasto-plastic behaviors. In addition, the volumetric part of the plastic deformation is described with the corrector of the volumetric part of the elastic logarithmic strain. It offers a new and sound kinematic approach to deal with non-isochoric plasticity. We also use the GTN function as an example to demonstrate the use of the kinematic relation as well as the implementation of the implicit algorithm.

*Keywords:* non-isochoric plasticity, large-strain, void growth, GTN model, elastic corrector, logarithmic strain

---

## 1. Introduction

Non-isochoric plastic deformation mechanisms like void growth are very common. On the other hand, nowadays porous materials are widely used and exist in different forms, for example, mechanical metamaterials are mostly porous materials in the continuum scale. In addition, pores are the one of the most common defects in material manufacture (Gao et al., 2020). The prediction of void evolution can be very important for describing the deformation and fracture mechanisms of such materials. One main approach is by using the void growth models, which have two important aspects: one is the void evolution rule, another one is the large-strain kinematics, especially the relation between the volume change due to void evolution and the strain type variable. The focus of this work is the latter.

---

\*Corresponding author.

*Email address:* fco.montans@upm.es (Francisco Javier Montáns)

The Gurson-Tvergaard-Needleman (GTN) type yield function is one of the most widely used void evolution rule (Gurson, 1977; Tvergaard and Needleman, 1984; Needleman and Tvergaard, 1987). There have been excessive extensions of the model, e.g., to include the description of the nucleation and coalescence of the voids (Chu and Needleman, 1980; Thomson et al., 2003; Pardoen and Hutchinson, 2000), to account for the low or high stress triaxiality case (Malcher et al., 2014; Wu et al., 2019; Xue, 2008; Vadillo et al., 2016), to determine parameters (Zhang et al., 2021b; He et al., 2021; Yin et al., 2022), to avoid mesh-dependance by non-local models (Hütter et al., 2013; Bergo et al., 2021), to include anisotropic yield criteria (Chen and Dong, 2009), to consider cyclic loading conditions (Wu et al., 2024), and so on, however, there has not been much study on the framework, especially there has not been an over-all sound and simple framework for the large strain implementation. Most of the implementations still use the small-strain formulations (Thomson et al., 2003; Malcher et al., 2014; Wu et al., 2019; Vadillo et al., 2016; Zhang et al., 2021b; He et al., 2021; Wu et al., 2024), which is not always appropriate, especially when void growth causes localization of deformation which can easily exceed the small-strain regime. Not only for the GTN models, no matter which void evolution rule is used, the large-strain framework is fundamental for predicting accurately and efficiently the void evolution.

Similar to the large-strain formulations for isochoric plasticity, in the previous works, the large-strain kinematics of void growth models usually lacks accuracy and generality, and the following are some examples. Hutter et al. used a hypoelastic approach to relate the Jaumann stress rate and the deformation rate (Hütter et al., 2013), similar works can be found in (Nasir et al., 2021; Tuhami et al., 2022; Mansouri et al., 2014; Seupel et al., 2020; Orsini and Zikry, 2001), even though hypoelastic formulations are known to be problematic (Simo and Pister, 1984). Chen et al. used the plastic logarithmic stains and its work conjugate to calculate the dissipation (Chen et al., 2022), which implementation is also not overall sound, because instead of the Kroner-Lee multiplicative decomposition, the authors simply used an additive decomposition of total material logarithmic strain to get the elastic and plastic strain, a similar treatment can be found in (Zhang et al., 2018). Quinn et al. adopted the conventional framework of crystal plasticity (Quinn et al., 1997), which implementation is arguably complicated and involves several approximations that result in constraints on the amount of elastic strain and elastoplastic behaviors, and this approach can also be found in similar models that employ crystal plasticity (Ha and Kim, 2010; Potirniche et al., 2007; Guo et al., 2020; Shang et al., 2020; Ling et al., 2018). Mahnken in (Mahnken, 1999) followed the work of Simo (Simo, 1992) and used the formulation with Lie derivative of the elastic left Cauchy-Green tensor, which is only valid for isotropic material and arguably lacks simplicity. Bergo et al. used the Cauchy stress and the plastic deformation rate to calculate the plastic dissipation (Bergo et al., 2021), which is also problematic because the work conjugate of the deformation rate is the Kirchhoff stress.

Recently, we proposed a fully hyperelastic formulation for isochoric plastic defor-

mation that use elastic correctors (Latorre and Montáns, 2018; Zhang and Montáns, 2019; Zhang et al., 2021a), it maintains the Kroner-Lee multiplicative decomposition and uses the logarithmic stain for achieving an additive structure. The framework does not have any constraint on the amount of the elastic strain and the form of elasto-plastic behaviors and it allows a simple implementation of a fully hyperelastic formulation. In addition, it is consistent and parallel to continuum elastoplasticity and crystal plasticity. In this work, we extend our framework to void growth models, moreover, we propose a new kinematic relation that relates the void evolution with the elastic logarithmic strain. For simplicity, we use the classic GTN yield function as the void evolution rule. Please note that other evolution rules can also be applied. In the following part, we first introduce the kinematic relations; and then the implementation of the GTN model within this framework; we further demonstrate the soundness and robustness of the implemented model by several numerical examples.

## 2. Void growth kinematic relations

The material consists of a solid matrix with volume  $V_m$  which we consider identical to the reference volume  $V$ , and a volume of voids of  $v_o$ . The current, locally unloaded volume is  $V + v_o \equiv V_m + v_o$ , whereas an elastically deformed incremental volume  $v_e$  gives a deformed volume of the continuum equal to

$$v = V_m + v_o + v_e \quad (1)$$

so we can write the functional dependence  $v_e = v_e(v, v_o) = (v - V_m) - v_o$ , which in rate form is  $\dot{v}_e = \dot{v} - \dot{v}_o$ . Since pure plastic flow in the matrix is considered isochoric, the change of volume  $v_p$  due to plastic flow is assumed to come only from the voids increment, i.e.  $v_p = v_o$ . Consider the deformation gradient  $\mathbf{X}$ . The change of volume is given by the Jacobian of the deformation, i.e.  $J = \det(\mathbf{X})$  which is

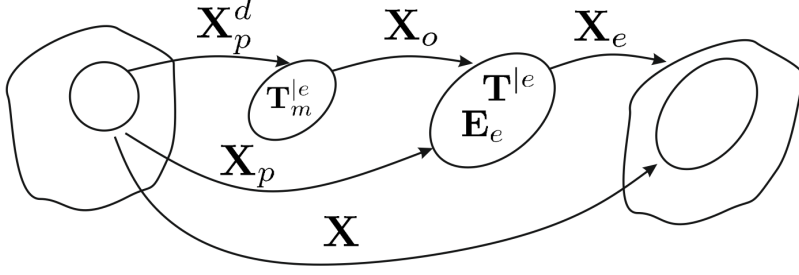
$$J = \frac{v}{V} = \frac{V_m + v_o + v_e}{V_m} = \left( \frac{V_m + v_o + v_e}{V_m + v_o} \right) \left( \frac{V_m + v_o}{V_m} \right) = J_e J_o \equiv J_e J_p \quad (2)$$

where note that we obtain the multiplicative decomposition  $J = J_e J_o \equiv J_e J_p$ , which is the volumetric counterpart of

$$\mathbf{X} \equiv \mathbf{X}_e \underbrace{\mathbf{X}_o \mathbf{X}_p^d}_{=: \mathbf{X}_p} = \mathbf{X}_e \mathbf{X}_p \Rightarrow J = \det(\mathbf{X}) = \det(\mathbf{X}_e) \det(\mathbf{X}_p) = J_e J_p \quad (3)$$

Even though they have some different nature, note that we incorporate  $\mathbf{X}_o = J_o^{1/3} \mathbf{I}$  corresponding to the void growth to  $\mathbf{X}_p^d$ , corresponding to the (isochoric) plastic deformation of the matrix. We define the void ratio as  $f(v_o) = v_o / (V_m + v_o)$ . Then, using  $J_o \equiv J_p = (V_m + v_o) / V_m$

$$1 - \frac{1}{J_p} = \frac{J_p - 1}{J_p} = \frac{V_m + v_o}{V_m + v_o} - \frac{V_m}{V_m + v_o} = \frac{v_o}{V_m + v_o} = f \quad (4)$$



and

$$1 - f = \frac{V_m + v_o}{V_m + v_o} - \frac{v_o}{V_m + v_o} = \frac{V_m}{V_m + v_o} = J_o^{-1} \quad (5)$$

and

$$\dot{f} = \frac{df}{dv_o} = \frac{\dot{v}_o}{V_m + v_o} - \frac{v_o \dot{v}_o}{(V_m + v_o)^2} = \frac{V_m \dot{v}_o}{(V_m + v_o)^2} \quad (6)$$

so we obtain the following expression useful below

$$\frac{\dot{f}}{1 - f} = \frac{\dot{v}_o}{V_m + v_o} = \frac{\dot{J}_p}{J_p} \quad (7)$$

The Jacobian of the elastic deformation is

$$J_e = \frac{V_m + v_o + v_e}{V_m + v_o} \quad (8)$$

$$\dot{J}_e J_e^{-1} = \frac{\dot{v}_e}{V_m + v_o} + \frac{\dot{v}_o}{V_m + v_o} = \frac{\dot{v}_e}{V_m + v_o + v_e} + \frac{\dot{v}_o}{V_m + v_o + v_e} \quad (9)$$

The trial elastic rate of deformation, i.e. when the plastic flow is frozen is

$$\left. \frac{d}{dt} (J) \right|_{j_p = \dot{v}_o = 0} = \left. \frac{d}{dt} \left( \frac{V_m + v_o + v_e}{V_m} \right) \right|_{j_p = \dot{v}_o = 0} = \frac{\dot{v}_e}{V_m} \quad (10)$$

so

$$\left. \frac{d}{dt} (J) \right|_{j_p = \dot{v}_o = 0} J^{-1} = \frac{\dot{v}_e}{V_m} \frac{V_m}{V_m + v_o + v_e} = \frac{\dot{v}_e}{V_m + v_o + v_e} \quad (11)$$

Note that

$$\dot{J}_e \Big|_{\dot{v}_o = 0} J_e^{-1} = \frac{\dot{v}_e}{V_m + v_o} \frac{V_m + v_o}{V_m + v_o + v_e} = \frac{\dot{v}_e}{V_m + v_o + v_e} = \left. \frac{d}{dt} (J) \right|_{j_p = \dot{v}_o = 0} J^{-1} \quad (12)$$

hence, we obtain the relation consistent with the definition of elastic trial rate

$$\frac{\dot{J}_e \Big|_{\dot{v}_o = j_p = 0}}{J_e} = \frac{\dot{J} \Big|_{\dot{v}_o = j_p = 0}}{J} \Leftrightarrow \text{tr} \dot{E}_e^v = \dot{E}^v \Big|_{\dot{v}_o = 0} \quad (13)$$

Therefore, considering the case of only internal evolution, so  $\dot{v} = 0$ , we have

$$\left. \frac{d}{dt} (J_e J_p) \right|_{\dot{v}=0} = \dot{J}_e J_p + J_e \dot{J}_p = 0 \quad (14)$$

we can also write

$$\left[ \frac{d}{dt} (J_e J_p) \right]_{\dot{v}=0} (J_e J_p)^{-1} = 0 = \left. \frac{\dot{J}_e J_p + J_e \dot{J}_p}{J_e J_p} \right|_{\dot{v}=0} = \left. \frac{\dot{J}_e}{J_e} \right|_{\dot{v}=0} + \frac{\dot{J}_p}{J_p} \quad (15)$$

which means that, by definition of corrector rate —note that  $\dot{J}_p J_p^{-1}$  does not depend on  $v$ , but only on  $v_o$

$${}^{ct} \dot{E}_e^v = \left. \frac{\dot{J}_e}{J_e} \right|_{\dot{v}=0} = - \frac{\dot{J}_p}{J_p} \quad (16)$$

Hence

$$\frac{\dot{J}_e}{J_e} = \dot{E}_e^v = \left. \dot{E}_e^v \right|_{\dot{v}_o=0} + \left. \dot{E}_e^v \right|_{\dot{v}=0} = {}^{tr} \dot{E}_e^v + {}^{ct} \dot{E}_e^v = \left. \frac{\dot{J}}{J} \right|_{\dot{v}_o=J_p=0} - \frac{\dot{J}_p}{J_p} \quad (17)$$

Then we obtain the following relation, *of purely kinematic nature, obtained by a simple relation of volumes,*

$$- {}^{ct} \dot{E}_e^v = \frac{\dot{J}_p}{J_p} \equiv \frac{\dot{J}_o}{J_o} = \frac{\dot{v}_o}{V_m + v_o} = \frac{\dot{f}}{1-f} \quad (18)$$

so we obtain a similar relation as in small strains, namely  $tr(\dot{\epsilon}_p) = \dot{f}/(1-f)$ , c.f. Eqs.(6) of (Gholipour et al., 2019), see also (Malcher et al., 2013, 2014; Bergo et al., 2021; Zhang et al., 2021b), but with the interpretation of logarithmic elastic corrector rate, and with the use of Jacobians. This is an accurate function, not got by using the mass conservation principle in an approximate way by neglecting the volume change due to elastic deformation like in small strains. Furthermore, note that this is *not* a constitutive relation, but a kinematic one *that must always hold*. Then,  $\dot{f}$  is due to void change of any nature (i.e. including due to nucleation and shear). In fact, if we consider different contributions ( $\dot{f}_g$  is due to void growth, and  $\dot{f}_n$  and  $\dot{f}_s$  are due to nucleation and shear),  $\dot{f} = \dot{f}_g + \dot{f}_n + \dot{f}_s$ , we get

$$- {}^{ct} \dot{E}_e^v = \frac{\dot{f}_g + \dot{f}_n + \dot{f}_s}{1-f} = \frac{\dot{f}_g}{1-f} + \frac{\dot{f}_n}{1-f} + \frac{\dot{f}_s}{1-f} = - {}^{ct,g} \dot{E}_e^v - {}^{ct,n} \dot{E}_e^v - {}^{ct,s} \dot{E}_e^v \quad (19)$$

which consists of a corrector contribution of elastic volumetric strains due to growth  ${}^{ct,g} \dot{E}_e^v$ , one due to nucleation of new voids  ${}^{ct,n} \dot{E}_e^v$  and one due to shear interaction effects  ${}^{ct,s} \dot{E}_e^v$ .

Consider now the change of volume of a void of volume  $v_o$  and radius  $r$ . Then,  $v_o = \frac{4}{3}\pi r^3$  and  $\dot{v}_o/v_o = 3\dot{r}/r$ . Then

$$\frac{\dot{v}_o}{v_o} \frac{v_o}{V + v_o} = 3 \frac{\dot{r}}{r} f = \dot{J}_p J_p^{-1} = - {}^{ct} \dot{\mathbf{E}}_e^v \quad (20)$$

The equation (18) stands regardless of the constitutive rule used. For example, when the void growth rule defined by Rice and Tracey is used, neglecting for the moment the influence of the Lode angle, the following expression for the growth rate of the void is given as a function of the pressure  $p$  and the yield stress in the matrix  $\kappa$

$$\frac{\dot{r}}{r} = \dot{\gamma} a \sinh \left( \frac{3p}{2\kappa} \right) \quad (21)$$

where  $a$  is a parameters ( $\approx 0.56$ ), and  $\dot{\gamma}$  is the rate of effective strain (uniaxial equivalent). Since we interpret  $\kappa$  as a Kirchhoff-like yield stress in the intermediate configuration,  $p$  is a Kirchhoff-like pressure ( $p/J$  is the Cauchy pressure, but note that for the ratio  $p/\kappa$  it is irrelevant if both stresses are of the same type). Hence, using Eqs. (20) and (21)

$$- {}^{ct,g} \dot{\mathbf{E}}_e^v = 3\dot{\gamma} a f \sinh \left( \frac{3p}{2\kappa} \right) \Rightarrow - {}^{ct,g} \dot{\mathbf{E}}_e^v = \frac{1}{3} {}^{ct,g} \dot{\mathbf{E}}_e^v \mathbf{I} = \dot{\gamma} a f \sinh \left( \frac{3p}{2\kappa} \right) \mathbf{I} \quad (22)$$

### 3. Stored energy and dissipation

The power in the solid by a volume vector load  $\mathbf{b}$  and surface traction  $\mathbf{t}$  is ((Latorre and Montáns, 2016))

$$P_V = \int_v \mathbf{b} \cdot \dot{\mathbf{u}} dv + \int_s \mathbf{t} \cdot \dot{\mathbf{u}} ds = \int_V \mathbf{T} : \dot{\mathbf{E}} dV \quad (23)$$

where  $\mathbf{T}$  is the work-conjugate stresses for referential logarithmic stresses in the most general case. Note that  $V$  is here the reference volume. Then, if  $\Psi(\mathbf{E}_e)$  is the stored energy per reference volume (*i.e. the stored energy in the matrix per initial matrix volume*), function of the elastic referential strains  $\mathbf{E}_e = \frac{1}{2} \ln(\mathbf{X}_e^T \mathbf{X}_e)$ , then the dissipation per reference volume  $V$  is

$$\begin{aligned} \dot{\mathcal{D}}^p &= \mathcal{P} - \dot{\Psi} = \mathbf{T} : \dot{\mathbf{E}} - \frac{d\Psi}{d\mathbf{E}_e} : \dot{\mathbf{E}}_e \\ &= \mathbf{T} : \dot{\mathbf{E}} - \frac{d\Psi}{d\mathbf{E}_e} : \left( {}^{tr} \dot{\mathbf{E}}_e + {}^{ct} \dot{\mathbf{E}}_e \right) \end{aligned} \quad (24)$$

As usual, we consider the two possible cases, which correspond to the two partial derivatives considered, as a function of the two variables; recall  $\mathbf{E}_e(\mathbf{E}, \mathbf{X}_p)$ . The first one is the absence of dissipation, i.e.  $\dot{\mathbf{X}}_p = {}^{ct}\dot{\mathbf{E}}_e = \mathbf{0}$  and  $\dot{\mathbf{E}}_e \equiv {}^{tr}\dot{\mathbf{E}}_e$  and  $\mathcal{D}^p = 0$ , so

$$\mathbf{T} = \frac{d\Psi}{d\mathbf{E}_e} : \frac{\partial \mathbf{E}_e}{\partial \mathbf{E}} \Big|_{\dot{\mathbf{X}}_p=0} = \mathbf{T}^{|e} : \frac{\partial \mathbf{E}_e}{\partial \mathbf{E}} \Big|_{\dot{\mathbf{X}}_p=0} \quad (25)$$

where we have defined the internal stresses

$$\mathbf{T}^{|e} = \frac{d\Psi}{d\mathbf{E}_e} \quad (26)$$

which are defined in the *intermediate* (“unloaded”) *configuration*, which is common to that of the “elastic” strains  $\mathbf{E}^e$ . Recall that the mapping  $\partial \mathbf{E}_e / \partial \mathbf{E} |_{\dot{\mathbf{X}}_p=0}$  transforms the pull-back to the reference configuration, where  $\mathbf{T}$  lives. Noteworthy,  $\mathbf{T}$  for the case of isotropy and proportional loading are the Kirchhoff stresses  $\boldsymbol{\tau} = J\boldsymbol{\sigma}$ , where  $\boldsymbol{\sigma}$  are the Cauchy stresses.

As mentioned, the plastic deformation in the matrix is isochoric. There are two types of irreversible deformations. One is due to the isochoric plastic deformation of the matrix, given by  $\mathbf{X}_p^d$ , and one by void growth given by  $\mathbf{X}_o = J_o^{1/3}\mathbf{I}$ , which is in essence also a result of plastic flow in the matrix, but which manifests at the continuum level through volumetric deformations. It can be also interpreted as two modes of plastic deformation, one isochoric and the other one volumetric. The decomposition of the deformation gradient is

$$\mathbf{X} = \mathbf{X}_e \mathbf{X}_o \mathbf{X}_p^d \quad (= \mathbf{X}_e \mathbf{X}_p) \quad (27)$$

This decomposition defines two intermediate configurations, see Figure 2. The stress tensor  $\mathbf{T}^{|e}$  lives in the “elastically unloaded” configuration. However, that configuration includes the void growth. *If a von Mises yield criterion is applied to the matrix, the stresses should not be  $\mathbf{T}^{|e}$ , because the associated volume of reference is  $V + v_o$ . In other words, the voids do not store energy. Then, using Eq. (5)*

$$\mathbf{T}_m^{|e} := \frac{v_o + V_m}{V_m} \mathbf{T}^{|e} = J_o \mathbf{T}^{|e} = \frac{\mathbf{T}^{|e}}{(1-f)} \quad (28)$$

After Tvergaard (?) it is customary to include a sort of stress concentration factor  $q_1$  which amplifies the effect of the void ratio, i.e. the effective (or fictitious continuum-equivalent) stress in the matrix for plastic flow is

$$\mathbf{T}_m^{|e} = \frac{\mathbf{T}^{|e}}{(1 - q_1 f)} \quad (29)$$

where a typical value given is  $q_1 = 1.5$ , or  $q_1 = 1.25$  accounting for coalescence of voids. The dissipation in the matrix as given by the equivalent stress is

$$\dot{\mathcal{D}}_m^p = -\mathbf{T}_m^{|e} : {}^{ct}\dot{\mathbf{E}}_e \equiv -\mathbf{T}_m^{d|e} : {}^{ct}\dot{\mathbf{E}}_e^d =: \kappa \dot{\gamma} > 0 \quad (30)$$

where we considered  ${}^{ct}\dot{\mathbf{E}}_e$  be formed of a deviatoric and a volumetric part  ${}^{ct}\dot{\mathbf{E}}_e = {}^{ct}\dot{\mathbf{E}}_e^d + {}^{ct}\dot{\mathbf{E}}_e^v$  and so  $\mathbf{T}^e = \mathbf{T}^{d|e} + \mathbf{T}^{v|e}$ .

$${}^{ct}\dot{\mathbf{E}}_e = {}^{ct}\dot{\mathbf{E}}_e^d + {}^{ct}\dot{\mathbf{E}}_e^v \quad (31)$$

The parameter  $\kappa$  is the yield stress of the *matrix* material without voids, and  $\dot{\gamma}$  is an equivalent plastic strain in the matrix. Note that we can consider a constant yield stress  $\kappa$  or isotropic hardening given by  $\kappa(\gamma)$  or by  $\kappa(D^p)$ . We can write in this case the (associative) flow rule as

$$- {}^{ct}\dot{\mathbf{E}}_e^d = \sqrt{\frac{3}{2}} \dot{\gamma} \frac{\mathbf{T}_m^{d|e}}{\kappa} \quad (32)$$

so

$$\dot{D}_m^p - \kappa \dot{\gamma} = \left( \frac{1}{\kappa} \sqrt{\frac{3}{2}} \mathbf{T}_m^{d|e} : \mathbf{T}_m^{d|e} - \kappa \right) \dot{\gamma} = 0 \quad (33)$$

or, if we use the stresses at the continuum level, taking into account some porosity

$$\dot{D}_m^p - \kappa \dot{\gamma} = \left( \frac{1}{\kappa} \sqrt{\frac{3}{2}} \frac{\mathbf{T}^{d|e}}{(1 - q_1 f)} : \frac{\mathbf{T}^{d|e}}{(1 - q_1 f)} - \kappa \right) \dot{\gamma} = 0 \quad (34)$$

which, if  $\dot{\gamma} > 0$ , it is equivalent to

$$F^d = \frac{\frac{3}{2} \|\mathbf{T}^{d|e}\|^2}{\kappa^2} - (1 - q_1 f)^2 = 0 \quad (35)$$

Note that this is the expression of the Gurson yield function given by Tvergaard & Needleman (Tvergaard and Needleman, 1984) when there is no pressure influence, i.e. when the pressure does not increase the void fraction. It is often recognized that this function represents Lemaitre's damage model, from continuum damage mechanics, in which  $D := q_1 f$  is the Rabotnov damage variable.

#### 4. Example: the GTN model

In this work, we will focus on elaborating the use of the framework with the classic and widely used GTN yield function as the constitutive rule which has been extensively studied and used in modelling void growth. The previous models are commonly implemented with small-strain framework. GTN function is a yield function that relates the void growth rate with the isochoric plasticity deformation.

$$F = \frac{\frac{3}{2} \|\mathbf{T}^{d|e}\|^2}{\kappa^2} - (1 - q_1 f)^2 + 2q_1 f \left[ \cosh \left( q_2 \frac{3p}{2\kappa} \right) - 1 \right] = 0 \quad (36)$$

where  $q_1$  is a parameter that amplifies the effect of void ratio, and  $q_2$  is another parameter frequently set to  $q_2 = 1$ , and for the pressure of the continuum  $p = 0$  the term in



brackets vanishes. The parameter  $\kappa$  is the yield stress of the *matrix* material without voids.  $\mathbf{T}^{d|e}$  is de deviatoric stress of the continuum in the intermediate configuration. Noteworthy, the derivatives respect to the pressure and to  $\mathbf{T}^{d|e}$  are

$$\frac{\partial F}{\partial p} = \frac{3q_2(q_1f)}{\kappa} \sinh\left(\frac{3p}{2\kappa}q_2\right) \quad \text{and} \quad \frac{\partial F}{\partial \mathbf{T}^{d|e}} = 3\frac{\mathbf{T}^{d|e}}{\kappa^2} \quad (37)$$

Then, using the assumed associativity of ‘‘flow rule’’ for the continuum,

$$-{}^{ct,g}\dot{\mathbf{E}}_e = \dot{\lambda} \frac{dF}{d\mathbf{T}^{d|e}} = \dot{\lambda} \frac{dF}{d\mathbf{T}^{d|e}} : \frac{d\mathbf{T}^{d|e}}{d\mathbf{T}^{d|e}} + \dot{\lambda} \frac{dF}{dp} \frac{dp}{d\mathbf{T}^{d|e}} \quad (38)$$

$$\begin{aligned} &= 3\dot{\lambda} \frac{\mathbf{T}^{d|e}}{\kappa^2} + \dot{\lambda} \frac{q_2(q_1f)}{\kappa} \sinh\left(\frac{3p}{2\kappa}q_2\right) \mathbf{I} \\ &= -{}^{ct}\dot{\mathbf{E}}_e^d - {}^{ct,g}\dot{\mathbf{E}}_e^v = -{}^{ct}\dot{\mathbf{E}}_e^d - \frac{1}{3} {}^{ct,g}\dot{E}_e^v \mathbf{I} \end{aligned} \quad (39)$$

Here  $\lambda$  is the equivalent plastic strain in the continuum. Note that we can consider a constant yield stress  $\kappa$  or isotropic hardening given by  $\kappa(\lambda)$  or by the accumulated plastic strain. In this work, we add isotropic hardening by using a simple linear hardening function  $\kappa(\lambda) = \kappa_0 + H\lambda$ , with  $\kappa_0$  as the yield stress without hardening, and  $H$  as the hardening parameter.

The deviatoric and volumetric part of the corrector of elastic strain rate are:

$$-{}^{ct}\dot{\mathbf{E}}_e^d = 3\dot{\lambda} \frac{\mathbf{T}^{d|e}}{\kappa^2} \quad (40)$$

$$-{}^{ct}\dot{\mathbf{E}}_e^v = \frac{q_1q_2\dot{\lambda}f}{\kappa} \sinh\left(\frac{3p}{2\kappa}q_2\right) \mathbf{I} \quad (41)$$

Considering that from the kinematics, we already get (18), so when  ${}^{ct}\dot{E}_e^v \neq 0$ , we have

$$-{}^{ct}\dot{\mathbf{E}}_e^v = \frac{q_1q_2\dot{\lambda}f}{\kappa} \sinh\left(\frac{3p}{2\kappa}q_2\right) \mathbf{I} = \frac{1}{3} \frac{\dot{f}}{1-f} \mathbf{I} \quad (42)$$

It is noteworthy that when using current GTN yield function, when there is no volume change, there is no void evolution, so when only under isochoric deformation, there is no volume change of voids. A lot of improved GTN models have been proposed to account for the low stress triaxiality case (Malcher et al., 2014; Xue, 2008; Wu et al., 2019), but it is not the purpose of this work to extend a GTN model to account for specific cases.

#### 4.1. The algorithm for GTN model

The main calculation is carried out in the intermediate configuration. The integration algorithm is similar to that of small-strain formulation, only a post-processor would be added to change the stress and the elastoplastic tangent to the desired measure in the desired configuration. In the following part we are going to introduce the integration algorithm including isotropic hardening.

The trial of the logarithmic strain in the intermediate configuration of current step  ${}^{t+\Delta t}\mathbf{E}^{|e}$  can be obtained from the plastic deformation gradient of last step  ${}^t\mathbf{X}_p$  and the deformation gradient of current step  ${}^{t+\Delta t}\mathbf{X}$ :

$${}^{tr}\mathbf{X}_e = {}^{t+\Delta t}\mathbf{X}^t\mathbf{X}_p^{-1} \quad {}^{tr}\mathbf{E}^{|e} = \frac{1}{2} \ln({}^{tr}\mathbf{X}_e^T {}^{tr}\mathbf{X}_e) \quad (43)$$

To calculate the corrector  ${}^{ct}\mathbf{E}^{|e}$ , there are several alternative ways to carry out the local iterations, here we choose  ${}^{ct}E_e^v$  and  ${}^{ct}\mathbf{E}_e^d$  as the variables for the iterations. From the yield function (36) and the flow rule (38), we get the deviatoric (40) and volumetric part (41) of the corrector of the elastic strain rate, and if we represent  $\Delta\lambda$  with  ${}^{ct}E_e^v$ :

$$\Delta\lambda = -\frac{{}^{t+\Delta t}\kappa {}^{ct}E_e^v}{3q_1q_2 {}^{t+\Delta t}f \sinh\left(\frac{3q_2}{2} \frac{{}^{t+\Delta t}p}{{}^{t+\Delta t}\kappa}\right)} \quad (44)$$

By substituting the kinematic relation 18, we can get:

$$\Delta\lambda = \frac{{}^{t+\Delta t}\kappa \Delta f}{3q_1q_2 {}^{t+\Delta t}f (1 - {}^{t+\Delta t}f) \sinh\left(\frac{3q_2}{2} \frac{{}^{t+\Delta t}p}{{}^{t+\Delta t}\kappa}\right)} \quad (45)$$

After substituting it into (40), we get an residual function  $G$  for  ${}^{ct}\mathbf{E}_e^d$ . So for the local iterations, the two residual functions for the Newton-Raphson method can be:

$${}^{t+\Delta t}F = \frac{\frac{3}{2} \left\| {}^{t+\Delta t}\mathbf{T}^{d|e} \right\|^2}{{}^{t+\Delta t}\kappa^2} - (1 - q_1 {}^{t+\Delta t}f)^2 + 2q_1 {}^{t+\Delta t}f \left[ \cosh\left(\frac{3q_2}{2} \frac{{}^{t+\Delta t}p}{{}^{t+\Delta t}\kappa}\right) - 1 \right] = 0 \quad (46)$$

and

$${}^{t+\Delta t}G := {}^{ct}\mathbf{E}_e^d - \frac{{}^{ct}E_e^v}{{}^{t+\Delta t}\kappa q_1 q_2 {}^{t+\Delta t}f \sinh\left(\frac{3q_2}{2} \frac{{}^{t+\Delta t}p}{{}^{t+\Delta t}\kappa}\right)} {}^{t+\Delta t}\mathbf{T}^{d|e} = \mathbf{0} \quad (47)$$

Because  ${}^{t+\Delta t}\mathbf{T}^{|e} - {}^{t+\Delta t}\mathbb{A}^{|e} : ({}^{tr}\mathbf{E}^{|e} + {}^{ct}\mathbf{E}^{v|e} + {}^{ct}\mathbf{E}^{d|e}) = \mathbf{0}$ , and  ${}^{t+\Delta t}\mathbf{T}^{|e} = {}^{t+\Delta t}\mathbf{T}^{d|e} + {}^{t+\Delta t}p\mathbf{I}$ , we have:

$${}^{t+\Delta t}\mathbf{T}^{d|e} = {}^{tr}\mathbf{T}^{d|e} + {}^{t+\Delta t}\mathbb{A}^{|e} : {}^{ct}\mathbf{E}^{d|e} \quad (48)$$

$${}^{t+\Delta t}p\mathbf{I} = {}^{tr}\mathbf{T}^{v|e} + {}^{t+\Delta t}\mathbb{A}^{|e} : {}^{ct}\mathbf{E}^{v|e} \quad (49)$$

Since we assume that isotropic hardening is linear, we have:

$$\frac{d^{t+\Delta t} \kappa}{d\Delta\lambda} = H \quad (50)$$

$$\begin{aligned} \frac{\partial^{t+\Delta t} \kappa}{\partial^{ct} E^{v|e}} &= \frac{\partial^{t+\Delta t} \kappa}{\partial \Delta\lambda} \frac{\partial \Delta\lambda}{\partial^{ct} E^{v|e}} \\ &= \frac{\partial^{t+\Delta t} \kappa}{\partial \Delta\lambda} \left( \frac{\partial \Delta\lambda}{\partial^{t+\Delta t} f} \frac{\partial^{t+\Delta t} f}{\partial^{ct} E^{v|e}} + \frac{\partial \Delta\lambda}{\partial^{t+\Delta t} p} \frac{\partial^{t+\Delta t} p}{\partial^{ct} E^{v|e}} + \frac{\partial \Delta\lambda}{\partial^{t+\Delta t} \kappa} \frac{\partial^{t+\Delta t} \kappa}{\partial^{ct} E^{v|e}} \right) \end{aligned} \quad (51)$$

After rearranging it, we can get  $\frac{\partial^{t+\Delta t} \kappa}{\partial^{ct} E^{v|e}}$ :

$$\frac{\partial^{t+\Delta t} \kappa}{\partial^{ct} E^{v|e}} = \left( 1 - \frac{d^{t+\Delta t} \kappa}{d\Delta\lambda} \frac{\partial \Delta\lambda}{\partial^{t+\Delta t} \kappa} \right)^{-1} \left( \frac{d^{t+\Delta t} \kappa}{d\Delta\lambda} \frac{\partial \Delta\lambda}{\partial^{t+\Delta t} f} \frac{\partial^{t+\Delta t} f}{\partial^{ct} E^{v|e}} + \frac{d^{t+\Delta t} \kappa}{d\Delta\lambda} \frac{\partial \Delta\lambda}{\partial^{t+\Delta t} p} \frac{\partial^{t+\Delta t} p}{\partial^{ct} E^{v|e}} \right) \quad (52)$$

With the derivatives:

$$\begin{aligned} \frac{\partial \Delta\lambda}{\partial^{t+\Delta t} \kappa} &= \frac{\Delta f}{3q_1 q_2^{t+\Delta t} f(1-t+\Delta t) f \sinh\left(\frac{3q_2}{2} \frac{t+\Delta t p}{t+\Delta t \kappa}\right)} \\ &\quad + \frac{\Delta f \cosh\left(\frac{3q_2}{2} \frac{t+\Delta t p}{t+\Delta t \kappa}\right)^{t+\Delta t} p}{2q_1^{t+\Delta t} \kappa^{t+\Delta t} f(1-t+\Delta t) f \sinh^2\left(\frac{3q_2}{2} \frac{t+\Delta t p}{t+\Delta t \kappa}\right)} \end{aligned} \quad (53)$$

$$\begin{aligned} \frac{\partial \Delta\lambda}{\partial^{t+\Delta t} f} &= \frac{t+\Delta t \kappa}{3q_1 q_2^{t+\Delta t} f(1-t+\Delta t) f \sinh\left(\frac{3q_2}{2} \frac{t+\Delta t p}{t+\Delta t \kappa}\right)} \\ &\quad - \frac{\Delta f^{t+\Delta t} \kappa (1-2^{t+\Delta t} f)}{3q_1 q_2^{t+\Delta t} f^2 (1-t+\Delta t) f^2 \sinh\left(\frac{3q_2}{2} \frac{t+\Delta t p}{t+\Delta t \kappa}\right)} \end{aligned} \quad (54)$$

$$\frac{\partial \Delta\lambda}{\partial^{t+\Delta t} p} = - \frac{\Delta f \cosh\left(\frac{3q_2}{2} \frac{t+\Delta t p}{t+\Delta t \kappa}\right)}{2q_1^{t+\Delta t} f(1-t+\Delta t) f \sinh^2\left(\frac{3q_2}{2} \frac{t+\Delta t p}{t+\Delta t \kappa}\right)} \quad (55)$$

The derivatives of the first residual function  ${}^{t+\Delta t} F$  are:

$$\frac{\partial^{t+\Delta t} F}{\partial^{ct} \mathbf{E}^{d|e}} = \frac{\partial^{t+\Delta t} F}{\partial^{t+\Delta t} \mathbf{T}^{d|e}} \frac{\partial^{t+\Delta t} \mathbf{T}^{d|e}}{\partial^{ct} \mathbf{E}^{d|e}} \quad (56)$$

$$\begin{aligned} \frac{\partial^{t+\Delta t} F}{\partial^{ct} E^{v|e}} &= \frac{\partial^{t+\Delta t} F}{\partial^{t+\Delta t} p} \frac{\partial^{t+\Delta t} p}{\partial^{t+\Delta t} \mathbf{T}^{v|e}} \frac{\partial^{t+\Delta t} \mathbf{T}^{v|e}}{\partial^{ct} \mathbf{E}^{v|e}} \frac{\partial^{ct} \mathbf{E}^{v|e}}{\partial^{ct} E^{v|e}} \\ &\quad + \frac{\partial^{t+\Delta t} F}{\partial^{t+\Delta t} f} \frac{\partial^{t+\Delta t} f}{\partial^{ct} E^{v|e}} + \frac{\partial^{t+\Delta t} F}{\partial^{t+\Delta t} \kappa} \frac{\partial^{t+\Delta t} \kappa}{\partial^{ct} E^{v|e}} \end{aligned} \quad (57)$$

With the derivatives:

$$\frac{\partial^{t+\Delta t} F}{\partial^{t+\Delta t} \mathbf{T}^{d|e}} = \frac{3^{t+\Delta t} \mathbf{T}^{d|e}}{t+\Delta t \kappa^2} \quad (58)$$

$$\frac{\partial^{t+\Delta t} \mathbf{T}^{d|e}}{\partial^{ct} \mathbf{E}^{d|e}} = {}^{t+\Delta t} \mathbb{A}^{|e} \quad (59)$$

$$\frac{\partial^{t+\Delta t} F}{\partial^{t+\Delta t} p} = \frac{3q_1 q_2^{t+\Delta t} f}{t+\Delta t \kappa} \sinh\left(\frac{3q_2}{2} \frac{t+\Delta t p}{t+\Delta t \kappa}\right) \quad (60)$$

$$\frac{\partial^{t+\Delta t} p}{\partial^{ct} E^{v|e}} = \frac{\partial^{t+\Delta t} p}{\partial^{t+\Delta t} \mathbf{T}^{v|e}} \frac{\partial^{t+\Delta t} \mathbf{T}^{v|e}}{\partial^{ct} \mathbf{E}^{v|e}} \frac{\partial^{ct} \mathbf{E}^{v|e}}{\partial^{ct} E^{v|e}} = \frac{1}{9} \mathbf{I} : {}^{t+\Delta t} \mathbb{A}^{|e} : \mathbf{I} \quad (61)$$

$$\frac{\partial^{t+\Delta t} F}{\partial^{t+\Delta t} f} = 2q_1 \cosh\left(\frac{3q_2}{2} \frac{t+\Delta t p}{t+\Delta t \kappa}\right) - 2q_1^{t+\Delta t} f \quad (62)$$

$$\frac{\partial^{t+\Delta t} f}{\partial^{ct} E^{v|e}} = 1 / \left[ \frac{1}{t+\Delta t f - 1} - \frac{\Delta f}{(t+\Delta t f - 1)^2} \right] \quad (63)$$

$$\frac{\partial^{t+\Delta t} F}{\partial^{t+\Delta t} \kappa} = -\frac{3 \|\mathbf{T}^{d|e}\|^2}{t+\Delta t \kappa^3} - \frac{3q_1 q_2^{t+\Delta t} f^{t+\Delta t} p \sinh\left(\frac{3q_2}{2} \frac{t+\Delta t p}{t+\Delta t \kappa}\right)}{t+\Delta t \kappa^2} \quad (64)$$

The derivatives of the second residual function  ${}^{t+\Delta t} G$  are:

$$\frac{\partial^{t+\Delta t} G}{\partial^{ct} \mathbf{E}^{d|e}} = [{}^{t+\Delta t} \kappa q_1 q_2^{t+\Delta t} f \sinh\left(\frac{3q_2}{2} \frac{t+\Delta t p}{t+\Delta t \kappa}\right)] \mathbb{I} + \frac{\partial^{t+\Delta t} G}{\partial^{t+\Delta t} \mathbf{T}^{d|e}} \frac{\partial^{t+\Delta t} \mathbf{T}^{d|e}}{\partial^{ct} \mathbf{E}^{d|e}} \quad (65)$$

$$\frac{\partial^{t+\Delta t} G}{\partial^{ct} E^{v|e}} = -{}^{t+\Delta t} \mathbf{T}^{d|e} + \frac{\partial^{t+\Delta t} G}{\partial^{t+\Delta t} p} \frac{\partial^{t+\Delta t} p}{\partial^{ct} E^{v|e}} + \frac{\partial^{t+\Delta t} G}{\partial^{t+\Delta t} f} \frac{\partial^{t+\Delta t} f}{\partial^{ct} E^{v|e}} + \frac{\partial^{t+\Delta t} G}{\partial^{t+\Delta t} \kappa} \frac{\partial^{t+\Delta t} \kappa}{\partial^{ct} E^{v|e}} \quad (66)$$

With the derivatives:

$$\frac{\partial^{t+\Delta t} G}{\partial^{t+\Delta t} \mathbf{T}^{d|e}} = -{}^{ct} E_e^v \quad (67)$$

$$\frac{\partial^{t+\Delta t} G}{\partial^{t+\Delta t} p} = \frac{3}{2} q_1 q_2^{2t+\Delta t} f \cosh\left(\frac{3q_2}{2} \frac{t+\Delta t p}{t+\Delta t \kappa}\right) {}^{ct} \mathbf{E}_e^d \quad (68)$$

$$\frac{\partial^{t+\Delta t} G}{\partial^{t+\Delta t} f} = [{}^{t+\Delta t} \kappa q_1 q_2 \sinh\left(\frac{3q_2}{2} \frac{t+\Delta t p}{t+\Delta t \kappa}\right)] {}^{ct} \mathbf{E}_e^d \quad (69)$$

$$\frac{\partial^{t+\Delta t} G}{\partial^{t+\Delta t} \kappa} = q_1 q_2^{t+\Delta t} f \sinh\left(\frac{3q_2}{2} \frac{t+\Delta t p}{t+\Delta t \kappa}\right) {}^{ct} \mathbf{E}_e^d - \frac{3q_1 q_2^{2t+\Delta t} p^{t+\Delta t} f}{2^{t+\Delta t} \kappa} \cosh\left(\frac{3q_2}{2} \frac{t+\Delta t p}{t+\Delta t \kappa}\right) {}^{ct} \mathbf{E}_e^d \quad (70)$$

A plain Newton-Raphson method is used for the iteration, and the Jacobian matrix is:

$$\begin{bmatrix} \frac{\partial^{t+\Delta t} F}{\partial^{ct} \mathbf{E}^{d|e}} & \frac{\partial^{t+\Delta t} F}{\partial^{ct} E^{v|e}} \\ \frac{\partial^{t+\Delta t} G}{\partial^{ct} \mathbf{E}^{d|e}} & \frac{\partial^{t+\Delta t} G}{\partial^{ct} E^{v|e}} \end{bmatrix} \quad (71)$$

For updating the variables, an extra iteration is necessary when isotropic hardening is included. The variables of the local iterations are  $^{ct} \mathbf{E}^{d|e}$  and  $^{ct} E^{v|e}$ , and other variables obtained directly are  $\Delta f$  and  $^{t+\Delta t} \mathbf{T}^{|e}$ , but because  $\Delta \lambda$  and  $^{t+\Delta t} \kappa$  are dependant on each other, an extra iteration is needed to update them.

To get the analytical tangent, the key is to get the derivative of  $^{ct} \mathbf{E}_e^d$  and  $^{ct} \mathbf{E}_e^v$  to  $^{t+\Delta t} \mathbf{E}_e$ . Because  $^{t+\Delta t} \mathbf{E}_e = {}^{tr} \mathbf{E}_e + {}^{ct} \mathbf{E}_e$ , the derivative to  ${}^{tr} \mathbf{E}_e$  is:

$$\frac{d_0^{t+\Delta t} \mathbf{E}_e}{d {}^{tr} \mathbf{E}_e} = \mathbb{I} + \frac{d^{ct} \mathbf{E}_e}{d_0^{t+\Delta t} \mathbf{E}_e} \frac{d_0^{t+\Delta t} \mathbf{E}_e}{d {}^{tr} \mathbf{E}_e} \quad (72)$$

$$\frac{d_0^{t+\Delta t} \mathbf{E}_e}{d {}^{tr} \mathbf{E}_e} = (\mathbb{I} - \frac{d^{ct} \mathbf{E}_e}{d_0^{t+\Delta t} \mathbf{E}_e})^{-1} \quad (73)$$

$$\begin{aligned} \frac{d^{ct} \mathbf{E}_e}{d_0^{t+\Delta t} \mathbf{E}_e} &= \frac{d^{ct} \mathbf{E}_e^d}{d_0^{t+\Delta t} \mathbf{E}_e} + \frac{d^{ct} \mathbf{E}_e^v}{d_0^{t+\Delta t} \mathbf{E}_e} \\ &= \frac{d^{ct} \mathbf{E}_e^d}{d_0^{t+\Delta t} \mathbf{E}_e} + \frac{d^{ct} \mathbf{E}_e^v}{d^{t+\Delta t} f} \frac{d^{t+\Delta t} f}{d_0^{t+\Delta t} \mathbf{E}_e} \end{aligned} \quad (74)$$

First, for the volumetric part, because of the kinematic relation of the volumetric part 18, we obtain  $\frac{d^{ct} \mathbf{E}^{v|e}}{d^{t+\Delta t} f}$  as:

$$\frac{d^{ct} \mathbf{E}^{v|e}}{d^{t+\Delta t} f} = \frac{1}{3} \mathbf{I} \left( \frac{1}{{}^{t+\Delta t} f - 1} - \frac{\Delta f}{({}^{t+\Delta t} f - 1)^2} \right) \quad (75)$$

Second, for the deviatoric part, because  $-{}^{ct} \dot{\mathbf{E}}_e^d = 3\dot{\lambda} \frac{\mathbf{T}^{d|e}}{\kappa^2}$ , the derivative  $\frac{d^{ct} \mathbf{E}^{d|e}}{d_0^{t+\Delta t} \mathbf{E}_e}$  can be written as:

$$\begin{aligned} \frac{d^{ct} \mathbf{E}^{d|e}}{d_0^{t+\Delta t} \mathbf{E}_e} &= \frac{\partial^{ct} \mathbf{E}^{d|e}}{\partial^{t+\Delta t} \mathbf{T}^{d|e}} \frac{d^{t+\Delta t} \mathbf{T}^{d|e}}{d^{t+\Delta t} \mathbf{T}^{|e}} \frac{d^{t+\Delta t} \mathbf{T}^{|e}}{d_0^{t+\Delta t} \mathbf{E}_e} + \frac{\partial^{ct} \mathbf{E}^{d|e}}{\partial \Delta \lambda} \frac{d \Delta \lambda}{d_0^{t+\Delta t} \mathbf{E}_e} \\ &+ \frac{\partial^{ct} \mathbf{E}^{d|e}}{\partial^{t+\Delta t} \kappa} \frac{d^{t+\Delta t} \kappa}{d^{t+\Delta t} f} \frac{d^{ct} E^{v|e}}{d^{t+\Delta t} f} \frac{d^{t+\Delta t} f}{d_0^{t+\Delta t} \mathbf{E}_e} \end{aligned} \quad (76)$$

Here the key is to get  $\frac{d\Delta\lambda}{d_0^{t+\Delta t}\mathbf{E}_e}$  and  $\frac{d^{t+\Delta t}f}{d_0^{t+\Delta t}\mathbf{E}_e}$ , they can be calculated at the same time from the expression of  $\Delta\lambda$  and the yield function. Because:

$$\Delta\lambda = -\frac{{}^{t+\Delta t}\kappa^{ct}E^{v|e}}{3q_1q_2^{t+\Delta t}f\sinh(\frac{3q_2}{2}\frac{t+\Delta t p}{t+\Delta t\kappa})} \quad (77)$$

$$\begin{aligned} \frac{d\Delta\lambda}{d_0^{t+\Delta t}\mathbf{E}_e} &= \frac{\partial\Delta\lambda}{\partial^{ct}E^{v|e}}\frac{d^{ct}E^{v|e}}{d^{t+\Delta t}f}\frac{d^{t+\Delta t}f}{d_0^{t+\Delta t}\mathbf{E}_e} + \frac{\partial\Delta\lambda}{\partial^{t+\Delta t}f}\frac{d^{t+\Delta t}f}{d_0^{t+\Delta t}\mathbf{E}_e} \\ &+ \frac{\partial\Delta\lambda}{\partial^{t+\Delta t}\kappa}\frac{d^{t+\Delta t}\kappa}{d\Delta\lambda}\frac{d\Delta\lambda}{d_0^{t+\Delta t}\mathbf{E}_e} + \frac{\partial\Delta\lambda}{\partial^{t+\Delta t}p}\frac{d^{t+\Delta t}p}{d^{t+\Delta t}\mathbf{T}^{|e}}\frac{d^{t+\Delta t}\mathbf{T}^{|e}}{d_0^{t+\Delta t}\mathbf{E}_e} \end{aligned} \quad (78)$$

After rewriting (78), we can get:

$$\begin{aligned} \left(1 - \frac{\partial\Delta\lambda}{\partial^{t+\Delta t}\kappa}\frac{d^{t+\Delta t}\kappa}{d\Delta\lambda}\right)\frac{d\Delta\lambda}{d_0^{t+\Delta t}\mathbf{E}_e} &= \left(\frac{\partial\Delta\lambda}{\partial^{ct}E^{v|e}}\frac{d^{ct}E^{v|e}}{d^{t+\Delta t}f} + \frac{\partial\Delta\lambda}{\partial^{t+\Delta t}f}\right)\frac{d^{t+\Delta t}f}{d_0^{t+\Delta t}\mathbf{E}_e} \\ &+ \frac{\partial\Delta\lambda}{\partial^{t+\Delta t}p}\frac{d^{t+\Delta t}p}{d^{t+\Delta t}\mathbf{T}^{|e}}\frac{d^{t+\Delta t}\mathbf{T}^{|e}}{d_0^{t+\Delta t}\mathbf{E}_e} \end{aligned} \quad (79)$$

The derivatives used are 50 and:

$$\frac{\partial\Delta\lambda}{\partial^{ct}E^{v|e}} = -\frac{{}^{t+\Delta t}\kappa}{3q_1q_2^{t+\Delta t}f\sinh(\frac{3q_2}{2}\frac{t+\Delta t p}{t+\Delta t\kappa})} \quad (80)$$

$$\frac{\partial\Delta\lambda}{\partial^{t+\Delta t}f} = \frac{{}^{t+\Delta t}\kappa^{ct}E^{v|e}}{3q_1q_2^{t+\Delta t}f^2\sinh(\frac{3q_2}{2}\frac{t+\Delta t p}{t+\Delta t\kappa})} \quad (81)$$

$$\frac{\partial\Delta\lambda}{\partial^{t+\Delta t}\kappa} = -\frac{{}^{ct}E^{v|e}}{3q_1q_2^{t+\Delta t}f\sinh(\frac{3q_2}{2}\frac{t+\Delta t p}{t+\Delta t\kappa})} - \frac{{}^{ct}E^{v|e}\cosh(\frac{3q_2}{2}\frac{t+\Delta t p}{t+\Delta t\kappa})^{t+\Delta t}p}{2q_1^{t+\Delta t}\kappa^{t+\Delta t}f\sinh^2(\frac{3q_2}{2}\frac{t+\Delta t p}{t+\Delta t\kappa})} \quad (82)$$

$$\frac{\partial\Delta\lambda}{\partial^{t+\Delta t}p} = \frac{{}^{ct}E^{v|e}\cosh(\frac{3q_2}{2}\frac{t+\Delta t p}{t+\Delta t\kappa})}{2q_1^{t+\Delta t}f\sinh^2(\frac{3q_2}{2}\frac{t+\Delta t p}{t+\Delta t\kappa})} \quad (83)$$

If we separate the yield function (36) into two parts:

$$G_l := \frac{\frac{3}{2}\|{}^{t+\Delta t}\mathbf{T}^{d|e}\|^2}{t+\Delta t\kappa^2} \quad (84)$$

$$G_r := (1 - q_1^{t+\Delta t}f)^2 - 2q_1^{t+\Delta t}f\left[\cosh\left(\frac{3q_2}{2}\frac{t+\Delta t p}{t+\Delta t\kappa}\right) - 1\right] \quad (85)$$

Because  $G_l = Gr$ , it should always stand that:

$$\frac{dG_l}{d_0^{t+\Delta t} \mathbf{E}_e} = \frac{dGr}{d_0^{t+\Delta t} \mathbf{E}_e} \quad (86)$$

$$\begin{aligned} & \frac{\partial G_l}{\partial^{t+\Delta t} \mathbf{T}^{d|e}} \frac{d^{t+\Delta t} \mathbf{T}^{d|e}}{d^{t+\Delta t} \mathbf{T}_e} \frac{d^{t+\Delta t} \mathbf{T}_e}{d_0^{t+\Delta t} \mathbf{E}_e} + \frac{\partial G_l}{\partial^{t+\Delta t} \kappa} \frac{d^{t+\Delta t} \kappa}{d\Delta\lambda} \frac{d\Delta\lambda}{d_0^{t+\Delta t} \mathbf{E}_e} \\ &= \frac{\partial G_r}{\partial^{t+\Delta t} \kappa} \frac{d^{t+\Delta t} \kappa}{d\Delta\lambda} \frac{d\Delta\lambda}{d_0^{t+\Delta t} \mathbf{E}_e} + \frac{\partial G_r}{\partial^{t+\Delta t} p} \frac{d^{t+\Delta t} p}{d^{t+\Delta t} \mathbf{T}_e} \frac{d^{t+\Delta t} \mathbf{T}_e}{d_0^{t+\Delta t} \mathbf{E}_e} + \frac{\partial G_r}{\partial^{t+\Delta t} f} \frac{d^{t+\Delta t} f}{d_0^{t+\Delta t} \mathbf{E}_e} \end{aligned} \quad (87)$$

After rewriting (87), we can get:

$$\begin{aligned} \frac{\partial G_r}{\partial^{t+\Delta t} f} \frac{d^{t+\Delta t} f}{d_0^{t+\Delta t} \mathbf{E}_e} &= \left( \frac{\partial G_l}{\partial^{t+\Delta t} \kappa} \frac{d^{t+\Delta t} \kappa}{d\Delta\lambda} - \frac{\partial G_r}{\partial^{t+\Delta t} \kappa} \frac{d^{t+\Delta t} \kappa}{d\Delta\lambda} \right) \frac{d\Delta\lambda}{d_0^{t+\Delta t} \mathbf{E}_e} \\ &+ \frac{\partial G_l}{\partial^{t+\Delta t} \mathbf{T}^{d|e}} \frac{d^{t+\Delta t} \mathbf{T}^{d|e}}{d^{t+\Delta t} \mathbf{T}_e} \frac{d^{t+\Delta t} \mathbf{T}_e}{d_0^{t+\Delta t} \mathbf{E}_e} - \frac{\partial G_r}{\partial^{t+\Delta t} p} \frac{d^{t+\Delta t} p}{d^{t+\Delta t} \mathbf{T}_e} \frac{d^{t+\Delta t} \mathbf{T}_e}{d_0^{t+\Delta t} \mathbf{E}_e} \end{aligned} \quad (88)$$

The related derivatives are 50 and:

$$\frac{\partial G_l}{\partial^{t+\Delta t} \mathbf{T}^{d|e}} = \frac{3^{t+\Delta t} \mathbf{T}^{d|e}}{t+\Delta t \kappa^2} \quad (89)$$

$$\frac{\partial G_l}{\partial^{t+\Delta t} \kappa} = -\frac{3 \left\| \frac{t+\Delta t}{t+\Delta t} \mathbf{T}^{d|e} \right\|^2}{t+\Delta t \kappa^3} \quad (90)$$

$$\frac{\partial G_r}{\partial^{t+\Delta t} \kappa} = \frac{q_1 q_2^{t+\Delta t} f^{t+\Delta t} p \sinh\left(\frac{3q_2}{2} \frac{t+\Delta t p}{t+\Delta t \kappa}\right)}{t+\Delta t \kappa^2} \quad (91)$$

$$\frac{\partial G_r}{\partial^{t+\Delta t} f} = -2q_1 \cosh\left(\frac{3q_2}{2} \frac{t+\Delta t p}{t+\Delta t \kappa}\right) \quad (92)$$

$$\frac{\partial G_r}{\partial^{t+\Delta t} p} = -\frac{3q_1 q_2^{t+\Delta t} f \sinh\left(\frac{3q_2}{2} \frac{t+\Delta t p}{t+\Delta t \kappa}\right)}{t+\Delta t \kappa} \quad (93)$$

From (78) we can get:

$$\begin{aligned} \frac{d^{t+\Delta t} f}{d_0^{t+\Delta t} \mathbf{E}_e} &= \left( \frac{\partial G_r}{\partial^{t+\Delta t} f} \right)^{-1} \left( \frac{\partial G_l}{\partial^{t+\Delta t} \kappa} - \frac{\partial G_r}{\partial^{t+\Delta t} \kappa} \right) \frac{d^{t+\Delta t} \kappa}{d\Delta\lambda} \frac{d\Delta\lambda}{d_0^{t+\Delta t} \mathbf{E}_e} \\ &+ \left( \frac{\partial G_r}{\partial^{t+\Delta t} f} \right)^{-1} \left( \frac{\partial G_l}{\partial^{t+\Delta t} \mathbf{T}^{d|e}} \frac{d^{t+\Delta t} \mathbf{T}^{d|e}}{d^{t+\Delta t} \mathbf{T}_e} - \frac{\partial G_r}{\partial^{t+\Delta t} p} \frac{d^{t+\Delta t} p}{d^{t+\Delta t} \mathbf{T}_e} \right) \frac{d^{t+\Delta t} \mathbf{T}_e}{d_0^{t+\Delta t} \mathbf{E}_e} \end{aligned} \quad (94)$$

After substituting the expression of  $\frac{d^{t+\Delta t}f}{d_0^{t+\Delta t}\mathbf{E}_e}$  of (94) into (87), we can get the expression for  $\frac{d\Delta\lambda}{d_0^{t+\Delta t}\mathbf{E}_e}$  from:

$$\begin{aligned}
& \left[ 1 - \frac{\partial\Delta\lambda}{\partial^{t+\Delta t}\kappa} \frac{d^{t+\Delta t}\kappa}{d\Delta\lambda} - \left( \frac{\partial\Delta\lambda}{\partial^{ct}E^{v|e}} \frac{d^{ct}E^{v|e}}{d^{t+\Delta t}f} + \frac{\partial\Delta\lambda}{\partial^{t+\Delta t}f} \right) \left( \frac{\partial G_r}{\partial^{t+\Delta t}f} \right)^{-1} \left( \frac{\partial G_l}{\partial^{t+\Delta t}\kappa} - \frac{\partial G_r}{\partial^{t+\Delta t}\kappa} \right) \frac{d^{t+\Delta t}\kappa}{d\Delta\lambda} \right] \frac{d\Delta\lambda}{d_0^{t+\Delta t}\mathbf{E}_e} \\
& = \left( \frac{\partial\Delta\lambda}{\partial^{ct}E^{v|e}} \frac{d^{ct}E^{v|e}}{d^{t+\Delta t}f} + \frac{\partial\Delta\lambda}{\partial^{t+\Delta t}f} \right) \left( \frac{\partial G_r}{\partial^{t+\Delta t}f} \right)^{-1} \left( \frac{\partial G_l}{\partial^{t+\Delta t}\mathbf{T}^{d|e}} \frac{d^{t+\Delta t}\mathbf{T}^{d|e}}{d^{t+\Delta t}\mathbf{T}^{l|e}} - \frac{\partial G_r}{\partial^{t+\Delta t}p} \frac{d^{t+\Delta t}p}{d^{t+\Delta t}\mathbf{T}^{l|e}} \right) \frac{d^{t+\Delta t}\mathbf{T}^{l|e}}{d_0^{t+\Delta t}\mathbf{E}_e} \\
& + \frac{\partial\Delta\lambda}{\partial^{t+\Delta t}p} \frac{d^{t+\Delta t}p}{d^{t+\Delta t}\mathbf{T}^{l|e}} \frac{d^{t+\Delta t}\mathbf{T}^{l|e}}{d_0^{t+\Delta t}\mathbf{E}_e} \tag{95}
\end{aligned}$$

After getting  $\frac{d\Delta\lambda}{d_0^{t+\Delta t}\mathbf{E}_e}$ ,  $\frac{d^{t+\Delta t}f}{d_0^{t+\Delta t}\mathbf{E}_e}$  can be obtained from (94). Once  $\frac{d\Delta\lambda}{d_0^{t+\Delta t}\mathbf{E}_e}$  and  $\frac{d^{t+\Delta t}f}{d_0^{t+\Delta t}\mathbf{E}_e}$  are known,  $\frac{d^{ct}\mathbf{E}^{d|e}}{d_0^{t+\Delta t}\mathbf{E}_e}$  can be obtained from (76), thus  $\frac{d^{ct}\mathbf{E}_e}{d_0^{t+\Delta t}\mathbf{E}_e}$  can be obtained from (74), and  $\frac{d_0^{t+\Delta t}\mathbf{E}_e}{d^{tr}\mathbf{E}_e}$  can be obtained from (73). When  $\frac{d_0^{t+\Delta t}\mathbf{E}_e}{d^{tr}\mathbf{E}_e}$  is known,  ${}^{t+\Delta t}\mathbb{A}_{ep}^{|tr} = \frac{d^{t+\Delta t}\mathbf{T}^{l|tr}}{d^{tr}\mathbf{E}_e} \simeq \frac{d^{t+\Delta t}\mathbf{T}^{l|e}}{d^{tr}\mathbf{E}_e} = \frac{d^{t+\Delta t}\mathbf{T}^{l|e}}{d^{t+\Delta t}\mathbf{E}_e} : \frac{d^{t+\Delta t}\mathbf{E}_e}{d^{tr}\mathbf{E}_e} = {}^{t+\Delta t}\mathbb{A}^{l|e} : \frac{d^{t+\Delta t}\mathbf{E}_e}{d^{tr}\mathbf{E}_e}$  is known.

## 4.2. Numerical simulations

GTN model with current framework has been implemented as an user-material subroutine in our in-house finite element code DULCINEA. In the following numerical examples, we used single-element simulations to demonstrate the influence of the parameters  $q_1$  and  $q_2$ , and to discuss if the elastic constants of the continuum should change due to the change of the volume fraction of voids. We simulated the tensile test of a cube to show the influence of the hardening parameter  $H$ , as well as to show the robustness of the algorithm. Furthermore, we ran the tensile test of a necking bar, and prescribed the von Mises stress contours plot, the void volume fraction contour plot as well as the displacement-reaction force curve. The results are reasonable and the algorithm is robust.

### 4.2.1. Tensile test of a single element

Because the main purpose of this work is to introduce a new framework for the GTN model, instead of improving the model by adding extra rules for accounting for phenomena like void nucleation or void coalescence, only the GTN yield function is used as the constitutive rule. The parameters are only  $q_1$  and  $q_2$ . Following the traditional values given to  $q_1$  and  $q_2$ , the following is a brief study of the influence of the two parameters. Here no isotropic hardening is included, and the material parameters are listed in table 1.

Similar to previous GTN models, by increasing  $q_1$ , the void growth would be accelerated, and the flow stress would be decreased. By increasing  $q_2$ , the void growth rate would also be increased. When isotropic hardening is not included, the flow stress



$C_{11}$	$C_{12}$	$C_{44}$	$k_0$
269.4 GPa	115.4 GPa	77.0 GPa	96.0 MPa

Table 1: The elastic constants and the initial yield stress of the matrix material.

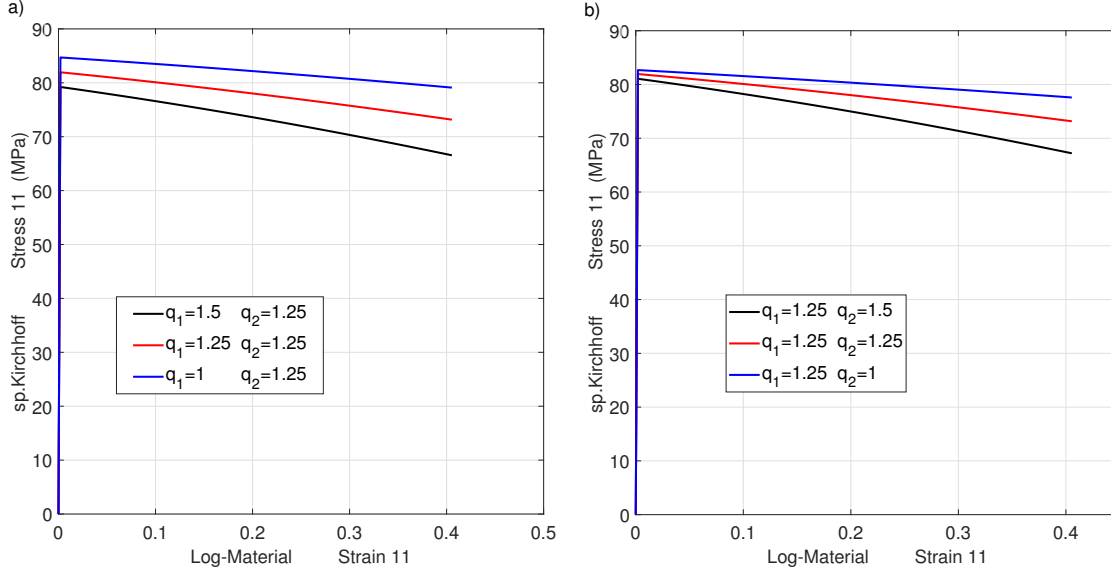


Figure 1: a) the influence of parameter  $q_1$ ; b) the influence of parameter  $q_2$

reflects the void volume fraction, so the influence of  $q_1$  and  $q_2$  is shown in figure 1. The simulation is a uniaxial tensile test with one element, with homogeneous boundary conditions with only the loading direction fully constraint. The initial volume fraction of void  $f_0$  is set as 0.1.

It should be noticed that because the elastic tangent of the void should be zero, the elastic tangent of the continuum should change according to the change of the volume fraction of the void. It is noticed that with current GTN model, this change does not influence the calculated flow stress and the volume fraction of the void, as shown in figure 2, however, the elastic strain as well as the stored energy are different in the two cases, so treating the elastic tangent of the continuum as constant in GTN models is problematic even though it does not change the results of flow stress or volume fraction of voids. For the simulation in the plot 2,  $q_1 = 1.25$ ,  $q_2 = 1.25$ .

#### 4.2.2. Tensile test of a cube

The sample is cubic with size length 1mm. Prescribed tensile displacement up to 0.5 mm is applied on the  $x$  direction, and homogeneous boundary condition, which

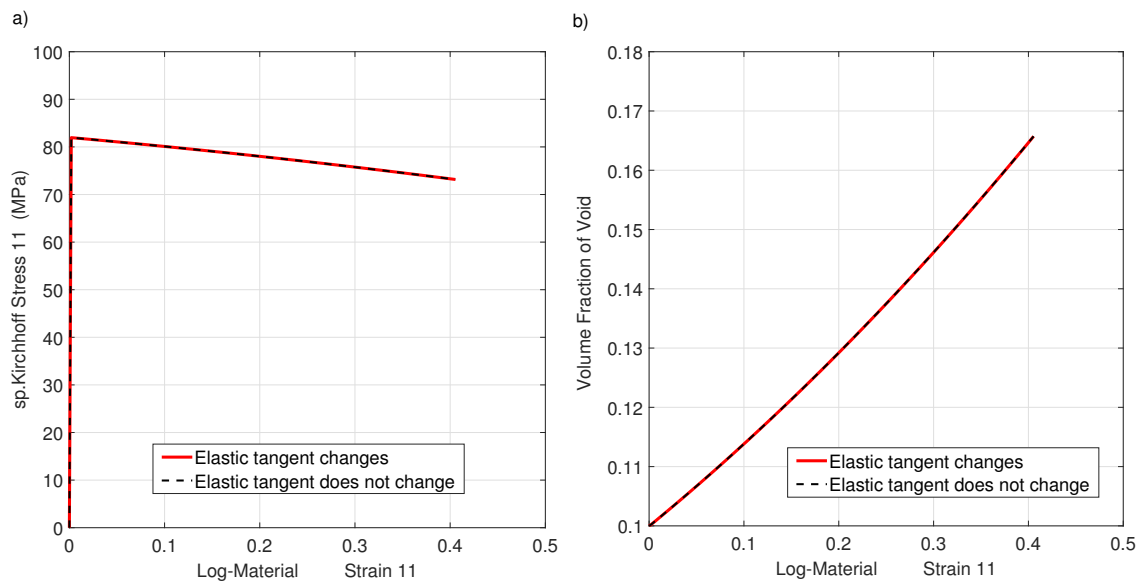


Figure 2: a) the calculated flow stress and b) the calculated volume fraction in the cases that the elastic tangent of the continuum changes and does not change according to the volume fraction of the voids

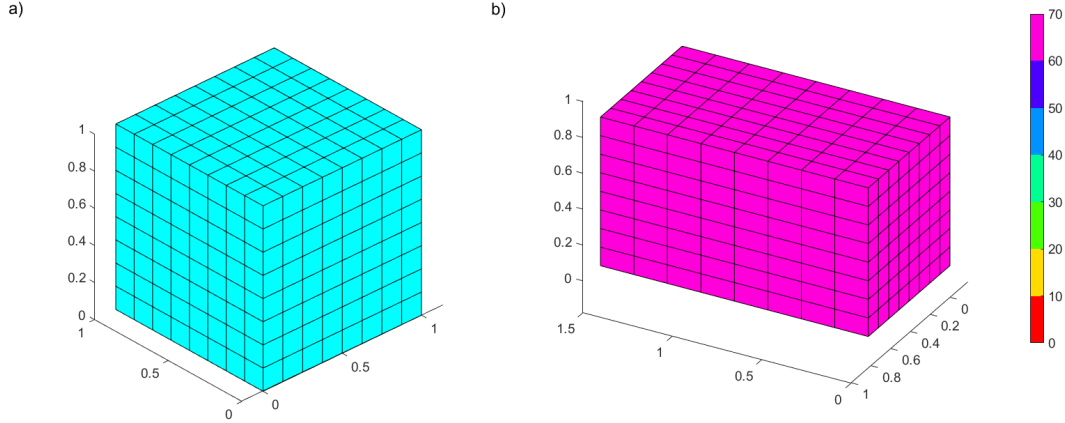


Figure 3: a) the undeformed shape of the cubic; b) the von Mises stress state of the deformed cubic.

Iteration	Residual norm			Energy norm		
	Step 75	Step 150	Step 225	Step 75	Step 150	Step 225
(1)	$5.417E + 02$	$5.486E + 02$	$5.649E + 02$	$1.566E + 01$	$1.587E + 01$	$1.635E + 01$
(2)	$4.517E - 02$	$3.583E - 02$	$2.937E - 02$	$5.069E - 07$	$3.091E - 07$	$1.988E - 07$
(3)	$5.085E - 05$	$3.411E - 05$	$2.404E - 05$	$2.060E - 12$	$3.105E - 12$	$6.069E - 12$

Table 2: Global convergence for several typical steps.

allows the sample to change freely on the other two directions. The undeformed and deformed sample are shown in figure 3. The element used is C3D20R, which has 20 nodes and 8 integration points. The total element number is 512. The total loading steps is 250. The material parameters used are listed in the table 1, with initial void volume fraction  $f_0 = 0.05$  and parameters for the model  $q_1 = 1$ ,  $q_2 = 1.25$ .

For this test, we set the isotropic hardening parameter  $H$  to different values, and compared the averaged stress-strain curves (a) of figure 4 as well as the void volume fraction-strain curves (b) of figure 4, from which we can conclude that for adding the isotropic hardening, when the yield stress of matrix  $\kappa$  is related to  $\lambda$ , it would not influence the void volume fraction.

In the table 2, we show the global convergence conditions of the force and energy of several typical steps for the case when no isotropic hardening is included.

#### 4.2.3. Tensile test of a plate with a hole

To further test the model, we ran the classic example of the tensile test of a thin plate with a hole in the middle. The thickness of the plate is 1 mm, and the other dimensions are shown in its undeformed shape in figure a) of 5. The element C3D20R is

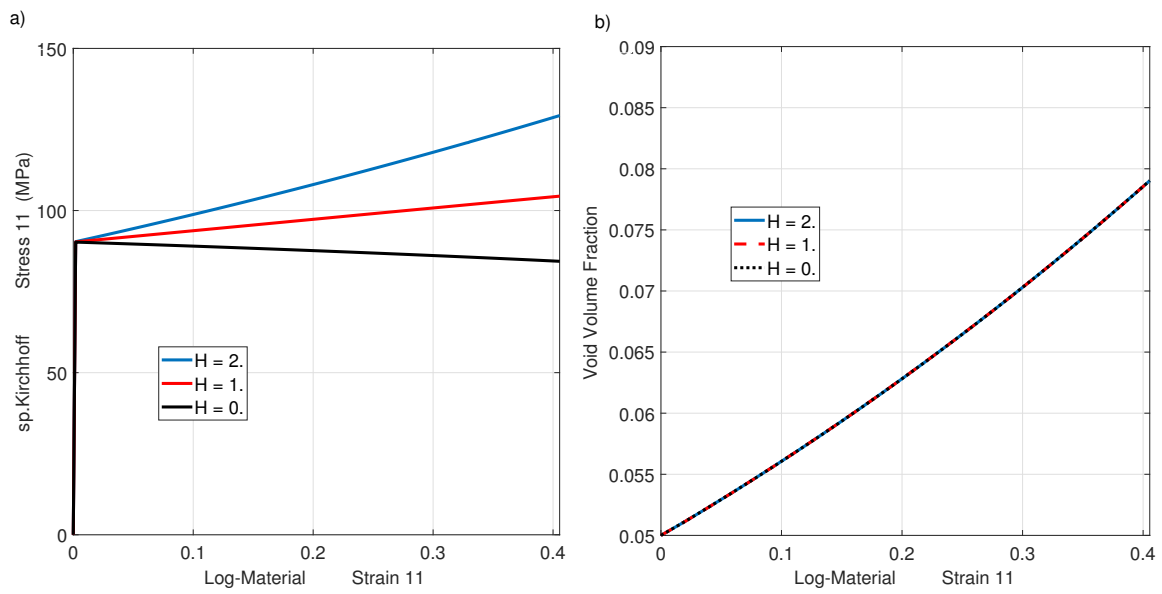


Figure 4: a) the averaged stress-strain curves for the cases when the hardening parameter  $H$  has different values; b) the averaged void volume fraction-strain curves for the cases when the hardening parameter  $H$  has different values

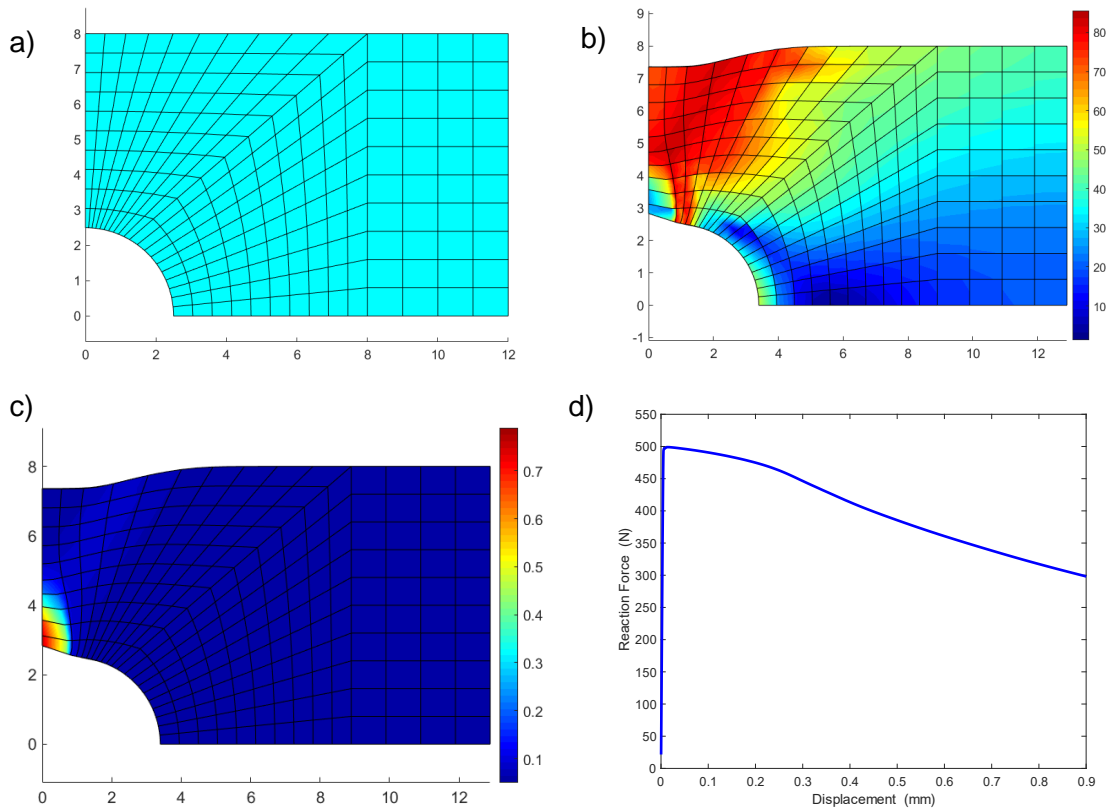


Figure 5: a) the dimensions of the undeformed plate; b) the deformed plate with contour plot of von Mises stress; c) the deformed plate with contour plot of the volume fraction of void; d) the displacement-reaction force plot of the loading end

used, because of symmetry, only 1/4 of the plate is modelled. To avoid early localization of deformation, a linear isotropic hardening with  $H = 0.85$  is added:  $\kappa = \kappa_0 + 0.85\lambda$ . For the model, the other material parameters used are also from the table 1, with initial void volume fraction  $f_0 = 0.05$  and parameters for the model  $q_1 = 1$ ,  $q_2 = 1.25$ .

The total tensile displacement is 7.5% of the length of the plate. The von Mises stress condition as well as the distribution of volume fraction of void are plotted in figure b) and c) of 5. The reaction force-displacement curve of the loading end of the specimen is plotted in d) of 5. For this work, we do not consider the coalescence of voids or the fracture criteria.

## 5. Conclusion

In this work, we demonstrate a new large-strain formulation for void evolution mechanisms. This formulation is an extension of our established framework that uses elastic correctors and logarithmic strains. It adopts the advantages of the framework, for example, it is fully hyperelastic and maintains the Kroner-Lee multiplicative decomposition; there is no constraint on the amount of the elastic strain and the form of the stored strain energy; both the theory and algorithm have an additive structure; it is consistent and parallel to continuum elastoplasticity as well as crystal plasticity. We proved that from the kinematics, we can get an accurate function that relates the evolution of the volume fraction of voids and the evolution of the corrector of the elastic volumetric strain  ${}^{ct}\dot{E}_e^v = -\frac{\dot{f}}{1-f}$ . We use the GTN yield function as an example of the void evolution rule to demonstrate the implementation of this formulation. With some numerical examples, we show that the implemented model can capture the features of the GTN model, and the algorithm is robust and simple.

## References

- Bergo, S., Morin, D., Sture Hopperstad, O., 2021. Numerical implementation of a non-local gtn model for explicit fe simulation of ductile damage and fracture. *International Journal of Solids and Structures* 219-220, 134–150.
- Chen, Y., Lorentz, E., Dahl, A., Besson, J., 2022. Simulation of ductile tearing during a full size test using a non local gurson–tvergaard–needleman (gtn) model. *Engineering Fracture Mechanics* 261, 108226.
- Chen, Z., Dong, X., 2009. The gtn damage model based on hill’48 anisotropic yield criterion and its application in sheet metal forming. *Computational Materials Science* 44, 1013–1021.
- Chu, C.C., Needleman, A., 1980. Void nucleation effects in biaxially stretched sheets. *Journal of Engineering Materials and Technology* 102, 249–256.
- Gao, X., Yuan, L., Fu, Y., Yao, X., Yang, H., 2020. Prediction of mechanical properties on 3d braided composites with void defects. *Composites Part B: Engineering* 197, 108164.
- Gholipour, H., Biglari, F., Nikbin, K., 2019. Experimental and numerical investigation of ductile fracture using gtn damage model on in-situ tensile tests. *International Journal of Mechanical Sciences* 164, 105170.
- Guo, H.J., Ling, C., Busso, E.P., Zhong, Z., Li, D.F., 2020. Crystal plasticity based investigation of micro-void evolution under multi-axial loading conditions. *International Journal of Plasticity* 129, 102673.

- Gurson, A.L., 1977. Continuum Theory of Ductile Rupture by Void Nucleation and Growth: Part I—Yield Criteria and Flow Rules for Porous Ductile Media. *Journal of Engineering Materials and Technology* 99, 2–15.
- Ha, S., Kim, K., 2010. Void growth and coalescence in f.c.c. single crystals. *International Journal of Mechanical Sciences* 52, 863–873.
- He, Z., Zhu, H., Hu, Y., 2021. An improved shear modified gtn model for ductile fracture of aluminium alloys under different stress states and its parameters identification. *International Journal of Mechanical Sciences* 192, 106081.
- Hütter, G., Linse, T., Mühlich, U., Kuna, M., 2013. Simulation of ductile crack initiation and propagation by means of a non-local gurson-model. *International Journal of Solids and Structures* 50, 662–671.
- Latorre, M., Montáns, F.J., 2016. Stress and strain mapping tensors and general work-conjugacy in large strain continuum mechanics. *Applied Mathematical Modelling* 40, 3938–3950.
- Latorre, M., Montáns, F.J., 2018. A new class of plastic flow evolution equations for anisotropic multiplicative elastoplasticity based on the notion of a corrector elastic strain rate. *Applied Mathematical Modelling* 55, 716–740.
- Ling, C., Forest, S., Besson, J., Tanguy, B., Latourte, F., 2018. A reduced micromorphic single crystal plasticity model at finite deformations. application to strain localization and void growth in ductile metals. *International Journal of Solids and Structures* 134, 43–69.
- Mahnken, R., 1999. Aspects on the finite-element implementation of the gurson model including parameter identification. *International Journal of Plasticity* 15, 1111–1137.
- Malcher, L., Andrade Pires, F., César de Sá, J., 2014. An extended gtn model for ductile fracture under high and low stress triaxiality. *International Journal of Plasticity* 54, 193–228.
- Malcher, L., Reis, F., Andrade Pires, F., César de Sá, J., 2013. Evaluation of shear mechanisms and influence of the calibration point on the numerical results of the gtn model. *International Journal of Mechanical Sciences* 75, 407–422.
- Mansouri, L.Z., Chalal, H., Abed-Meraim, F., 2014. Ductility limit prediction using a gtn damage model coupled with localization bifurcation analysis. *Mechanics of Materials* 76, 64–92.

- Nasir, M.W., Chalal, H., Abed-Meraim, F., 2021. Formability prediction using bifurcation criteria and gtn damage model. *International Journal of Mechanical Sciences* 191, 106083.
- Needleman, A., Tvergaard, V., 1987. An analysis of ductile rupture modes at a crack tip. *Journal of the Mechanics and Physics of Solids* 35, 151–183.
- Orsini, V., Zikry, M., 2001. Void growth and interaction in crystalline materials. *International Journal of Plasticity* 17, 1393–1417.
- Pardoen, T., Hutchinson, J., 2000. An extended model for void growth and coalescence. *Journal of the Mechanics and Physics of Solids* 48, 2467–2512.
- Potirniche, G., Horstemeyer, M., Ling, X., 2007. An internal state variable damage model in crystal plasticity. *Mechanics of Materials* 39, 941–952.
- Quinn, D., Connolly, P., Howe, M., McHugh, P., 1997. Simulation of void growth in wc-co hardmetals using crystal plasticity theory. *International Journal of Mechanical Sciences* 39, 173–183.
- Seupel, A., Hütter, G., Kuna, M., 2020. On the identification and uniqueness of constitutive parameters for a non-local gtn-model. *Engineering Fracture Mechanics* 229, 106817.
- Shang, X., Zhang, H., Cui, Z., Fu, M., Shao, J., 2020. A multiscale investigation into the effect of grain size on void evolution and ductile fracture: Experiments and crystal plasticity modeling. *International Journal of Plasticity* 125, 133–149.
- Simo, J., 1992. Algorithms for static and dynamic multiplicative plasticity that preserve the classical return mapping schemes of the infinitesimal theory. *Computer Methods in Applied Mechanics and Engineering* 99, 61–112.
- Simo, J., Pister, K., 1984. Remarks on rate constitutive equations for finite deformation problems: computational implications. *Computer Methods in Applied Mechanics and Engineering* 46, 201–215.
- Thomson, C., Worswick, M., Pilkey, A., Lloyd, D., 2003. Void coalescence within periodic clusters of particles. *Journal of the Mechanics and Physics of Solids* 51, 127–146.
- Tuhami, A.E.O., Feld-Payet, S., Quilici, S., Osipov, N., Besson, J., 2022. A two characteristic length nonlocal gtn model: Application to cup–cone and slant fracture. *Mechanics of Materials* 171, 104350.



- Tvergaard, V., Needleman, A., 1984. Analysis of the cup-cone fracture in a round tensile bar. *Acta Metallurgica* 32, 157–169.
- Vadillo, G., Reboul, J., Fernández-Sáez, J., 2016. A modified gurson model to account for the influence of the lode parameter at high triaxialities. *European Journal of Mechanics - A/Solids* 56, 31–44.
- Wu, H., Xu, W., Shan, D., Jin, B.C., 2019. An extended gtn model for low stress triaxiality and application in spinning forming. *Journal of Materials Processing Technology* 263, 112–128.
- Wu, H., Zhang, C., Yang, H., Zhuang, X., Zhao, Z., 2024. Extended gurson-tvergaard-needleman model considering damage behaviors under reverse loading. *International Journal of Mechanical Sciences* 272, 109196.
- Xue, L., 2008. Constitutive modeling of void shearing effect in ductile fracture of porous materials. *Engineering Fracture Mechanics* 75, 3343–3366. *Local Approach to Fracture (1986–2006): Selected papers from the 9th European Mechanics of Materials Conference.*
- Yin, Y., Ma, T., Han, Q., Lu, Y., Zhang, Y., 2022. Material parameters in the gtn model for ductile fracture simulation of g20mn5qt cast steels. *Journal of Materials in Civil Engineering* 34, 04021412.
- Zhang, M., Montáns, F.J., 2019. A simple formulation for large-strain cyclic hyperelasto-plasticity using elastic correctors. theory and algorithmic implementation. *International Journal of Plasticity* 113, 185–217.
- Zhang, M., Nguyen, K., Segurado, J., Montáns, F.J., 2021a. A multiplicative finite strain crystal plasticity formulation based on additive elastic corrector rates: Theory and numerical implementation. *International Journal of Plasticity* 137, 102899.
- Zhang, T., Lu, K., Mano, A., Yamaguchi, Y., Katsuyama, J., Li, Y., 2021b. A novel method to uniquely determine the parameters in gurson–tvergaard–needleman model. *Fatigue & Fracture of Engineering Materials & Structures* 44, 3399–3415.
- Zhang, Y., Lorentz, E., Besson, J., 2018. Ductile damage modelling with locking-free regularised gtn model. *International Journal for Numerical Methods in Engineering* 113, 1871–1903.